Electrochimica Acta 180 (2015) 712–721

Contents lists available at ScienceDirect

Electrochimica Acta

journal homepage: www.elsevier.com/locate/electacta

The Mechanism of Hydrogen Evolution During Anodic Polarization of Aluminium

M. Curioni*, F. Scenini

Corrosion and Protection Centre, The University of Manchester, Manchester, M13 9PL, United Kingdom

ARTICLE INFO

Article history:
Received 2 April 2015
Received in revised form 16 August 2015
Accepted 16 August 2015
Available online 3 September 2015

Keywords:
Aluminium
Corrosion
Hydrogen evolution
Negative difference effect

ABSTRACT

In this work, a model to account for the superfluous hydrogen evolution mechanism during anodic polarization of Al is proposed. The model is based on the assumption that the simultaneous presence of an anodic current, produced at some distance from the corrosion front, and of conditions that promote local depassivation such as, for example, the presence of chlorides, induces localized rupture of the pre-existing oxide/hydroxide film. This local depassivation leads to the formation of regions where the electrolyte is either in contact with the metal or separated only by a poorly protective salt film. Here, due to the large potential difference available, hydrogen evolves. The model is validated via electrochemical polarization assisted with in-situ image visualization of pure Al and Al/Cu system in experimental conditions that promote stable oxide film formation or induce local film rupture. Hydrogen streams from the active corrosion sites, increasing upon anodic polarization, are observed only in the presence of a depassivating media (chloride) and a remote cathodic current, provided either via galvanic coupling to copper or via external polarization.

1. Introduction

The aqueous corrosion behaviour of aluminium alloys is considerably affected by alloying elements and resulting microstructure. Although alloying additions generally increase the mechanical performance, they can also lead to the formation of a variety of second phase particles that might have a more or less noble electrochemical potential compared with the alloy matrix [1–3]. A typical example is formation of Cu rich second phases in series 2xxx which become predominant cathodic reaction sites. As a result of localization of the cathodic reaction, local pH variations and higher solubility of aluminium oxide with increased pH, a local dissolution of the adjacent alloy matrix is observed [3]. Such a phenomenon is often named 'trenching', and it can be seen as a localized anodic reaction, the dissolution of the matrix nearby a cathodic particle, induced by the localization of the cathodic reaction on the particle.

For metals having low oxidation potential, such as aluminium but also iron, chromium, magnesium and their alloys, the cathodic reaction of hydrogen evolution is thermodynamically possible during free corrosion, but the rate might be controlled by the presence of protective or partially protective oxide, hydroxide or mixed film on the metal surface. Thus, understanding the details of the process of hydrogen evolution at the active anodic regions on metal and alloys of practical technological interest is essential for the understanding of their corrosion behaviour and for the design of anticorrosion treatments and corrosion resistant alloys. Hydrogen evolution has been observed at the free corrosion potential from propagating pits on steel [4], aluminium [5–8] and aluminium alloys [9–12], and from the active corrosion front on magnesium and magnesium alloys [13–20]. When hydrogen evolution is observed from active corrosion sites at the free corrosion potential, increase in hydrogen evolution during anodic polarization is often reported. This observation is often named 'negative difference effect' or 'superfluous hydrogen evolution'. This terminology is due to the fact that the increase in the rate of hydrogen evolution during anodic polarization is contrary to the prediction from electrochemical theory, i.e. a decrease of the cathodic reaction (hydrogen evolution) rate with increasing anodic polarization [12,21,22]. The increase in hydrogen evolution with anodic polarization has been investigated in detail for aluminium, due to the wide use in batteries and sacrificial anodes, where the negative difference effect is detrimental, since it reduces the faradaic efficiency.

In order to rationalize the observed increase in hydrogen evolution during anodic polarization, various interpretations have been proposed and they can be broadly grouped in three categories: i) based on the assumption that metal cations with

* Corresponding author.
E-mail address: michele.curioni@manchester.ac.uk (M. Curioni).

http://dx.doi.org/10.1016/j.electacta.2015.08.076

lower valency are generated during anodic polarization [7,10,21,23,24], ii) based on the assumption that cluster of metal atoms detach from the corroding surface and oxidize in the electrolyte [22] iii) based on the idea that at the active corrosion front the surface film is absent or not protective and at these location hydrogen evolution is possible due to the large potential difference available [5,9].

The first interpretation is largely based on the comparison of the amount of metal oxidized (or hydrogen evolved) with the anodic charge applied to the corroding electrode [7,10]. Given that the oxidized metal (or the hydrogen evolved) generally exceeds what would be predicted by Faraday's law calculation for a valence of aluminium ions of three, it is postulated that some of the metal atoms oxidize to ions with a valence lower than three. Such low-valence ions then undergo further oxidation (by reducing a

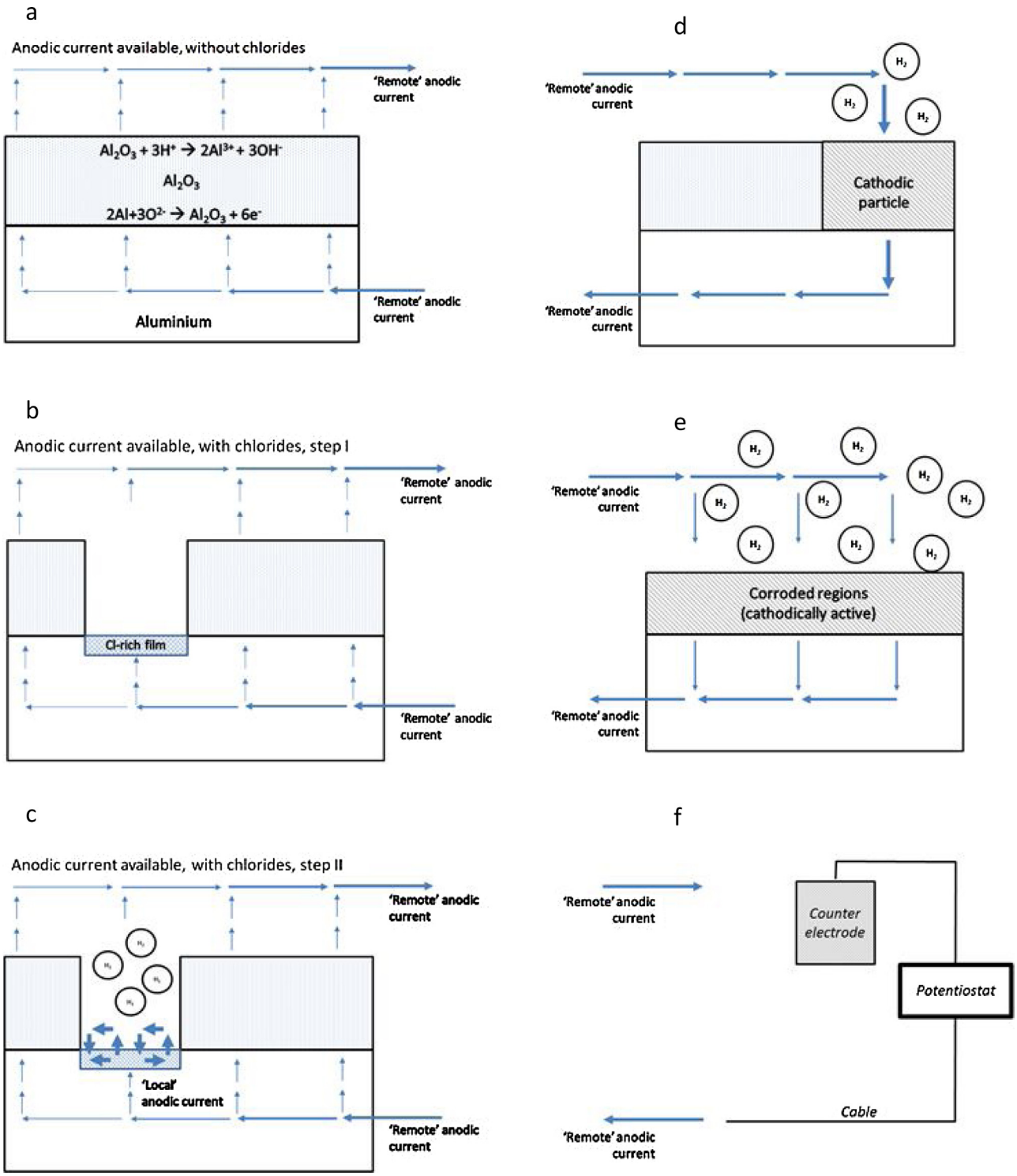

Fig. 1. a) Film growth due to the availability of 'remote' anodic current in the absence of chloride ions. b) Local depassivation in the presence of a 'remote' anodic current and of chloride ions, resulting in the formation of a salt film and c) hydrogen evolution at the corrosion front, producing local anodic current. Generation of 'remote' anodic current from d) cathodic particles on uncorroded regions or e) cathodically activated corroded regions or e) external circuit.

hydrogen ion) once detached from the electrode surface. Thus, an increase in anodic polarization produces an increase in low-valence ions and therefore an increase in the hydrogen evolved. This interpretation can accommodate the results from Faraday's law calculations, but the presence of low valence cations has not been proven directly. The second interpretation is based on the so called 'chunk' mechanism [22]. Specifically, it is assumed that, during anodic polarization, clusters of metal atoms (not oxidized) detach from the electrode surface and corrode in the electrolyte without being connected to the electrode. Once detached, they are no longer anodically polarized and therefore they can attain a lower potential and oxidize, with hydrogen evolution as cathodic reaction. Thus, increasing anodic polarization would increase the amount of metal clusters released, thereby increasing hydrogen evolution. Clearly, this mechanism can account for the excess of metal oxidized with respect to the applied anodic charge, since part of the oxidation process occurs on the electrically disconnected clusters. The possible presence of such metal clusters in the electrolyte is supported by visual observation of the electrolyte nearby the anodically electrode that appears cloudy. A third interpretation is based on the idea that at the local sites where the anodic reaction takes place, the surface film is absent or poorly protective and electrons can be exchanged from the metal to the electrolyte [4,5]. At these locations, due to the large potential difference between metal oxidation and hydrogen evolution, the latter takes place locally. This is possible because, at these active anodic sites, the potential at the metal surface is much lower than the macroscopic electrode potential, due to the high ohmic drop induced by the high value of local anodic current density. This mechanism is supported by the work of Borgeron et al. [5] who analysed the gases produced during corrosion of aluminium in various electrolytes containing KCl, KSCN, and $NaNO_3$. The presence of CH_4, H_2S N_2, NO and NH_3 after corrosion, suggests that the electrolyte species must have contacted directly the metal during corrosion.

For aluminium, it appears that superfluous hydrogen evolution is generally associated to pitting. For example, Drazic et al. [24] investigated the reaction of hydrogen evolution on aluminium on by using a rotating disk-ring arrangement where the disk was the aluminium specimen and the platinum ring was polarized to oxidise the newly formed hydrogen. By working in deaerated solutions, where the corrosion potential of the aluminium was well below the pitting potential, they revealed that hydrogen evolution decreased with anodic polarization (as expected for a cathodic reaction) until the pitting potential was reached. Above the pitting potential, the rate of hydrogen evolution increased abruptly. Hydrogen evolution above the pitting potential was also observed by Frankel [9] when investigating the growth of two-dimensional pits on thin aluminium films. Despic et al. [11], consistently found an increase in hydrogen evolution rate with increasing anodic polarization above the pitting potential and revealed that the addition of indium as alloying element reduced substantially this effect. Recently, Frankel et al. have investigated the anodic polarization behaviour of high-purity aluminium in very concentrated (12.1 M) HCl solutions, where generalized corrosion is expected. The potentiodynamic curves revealed an apparent active/passive transition, but the passive region was relatively small, extending only for about 100 mV. They also observed hydrogen evolution at the free corrosion potential, cessation of hydrogen evolution for polarization within the passive region, and increasing anodic hydrogen evolution for polarization at higher potentials [25].

As it is evident, the phenomenon of increased hydrogen evolution during anodic polarization of aluminium and aluminium alloys is well documented in the literature. However, a comprehensive view that is applicable to a corrosion situation is presently missing. Thus, the aim of this work is to investigate and rationalize this phenomenon that is somewhat symmetrical to the trenching described above. In fact, from the point of view of the electrical current within the electrode, the phenomenon of trenching can be seen as the generation of a local anodic current (associated to the dissolution of the matrix nearby the cathodic particle) induced by the presence of a 'remote' anodic site (located somewhere far from the particle) that provide the electrons to sustain the cathodic reaction on the particle.

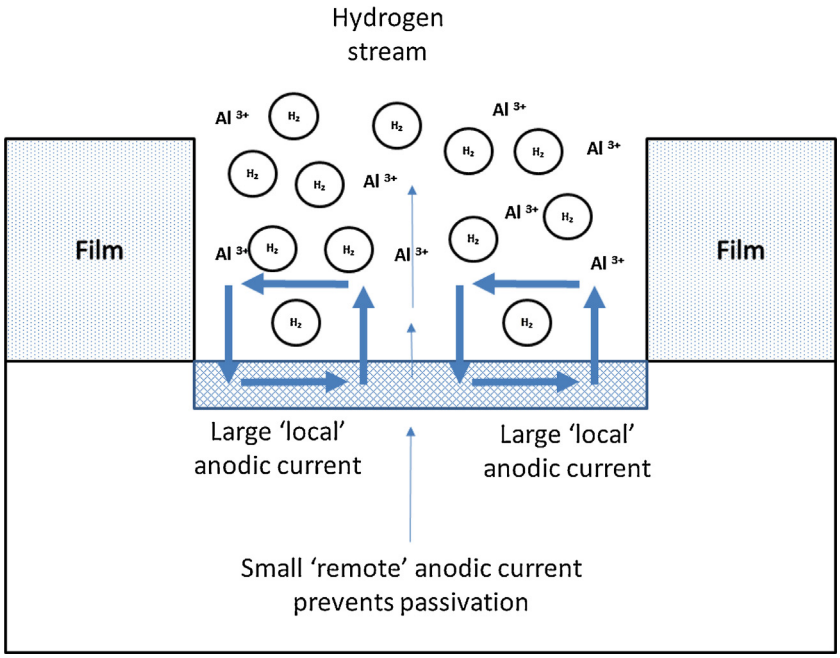

Fig. 2. Schematic representation of the current amplification process at the corrosion front. The 'remote' anodic current induces depassivation and maintains bare metal under a salt film. Hydrogen evolution induces a significant 'local' anodic current and hydrogen streams are observed. It's worth noting that local anode and local cathode are not necessarily spatially separated and that the aim of this schematic is to show the current amplification concept.

In this work the interaction between anodic and cathodic reaction and the resulting hydrogen evolution behaviour at the free corrosion potential and during anodic polarization, can be rationalized by using a model system based on aluminium and aluminium-copper electrodes. The reversible potential for aluminium oxidation is substantially lower than that for hydrogen evolution at all pH, therefore direct exposure of aluminium metal to an aqueous environment would result in hydrogen evolution. The stability of the aluminium oxide film can be tuned from very good (for example in sulphuric acid) to very poor (in sulphuric acid with the addition of NaCl). It is worth noting that in the sulphuric acid solution, due to the low pH, the oxide is in a dynamic equilibrium, progressively dissolving at the oxide/solution interface and growing at the metal/oxide interface following inward migration of oxygen ions and outward migration of aluminium ions [26–28]. Thus the driving force maintaining the dynamic equilibrium is provided by the potential difference between aluminium oxidation and hydrogen evolution occurring on cathodic sites such as impurities or second phase material. The cathodic activity of the electrode can be adjusted by macroscopic galvanic coupling with copper, mimicking the effect of noble impurities or pre-corroded regions exposing new intermetallics to the electrolyte. Finally, due to the macroscopic nature of the galvanic coupling in the model system, the effect of anodic polarization on the hydrogen evolved from corrosion front (on aluminium) or from cathodic regions (the copper) can be evaluated visually and directly. The model developed here is applicable for aluminium and its alloys. However, it can also be tuned to magnesium alloys after taking into consideration some fundamental differences between the two systems. The applicability to magnesium and magnesium alloys will be discussed in a future work.

2. Model of superfluous hydrogen evolution

It is proposed that the increased hydrogen evolution during anodic polarization and the development of hydrogen streams from the active corrosion site are mainly due to an increase in the cathodic activity at a site where the passivity due to the presence of a the oxide film is locally compromised and either the bare metal is somewhere in direct contact with the electrolyte or a thin film of chloride salt forms. The depassivation is caused by the simultaneous presence of an adequate local environment (chloride-containing, of low pH, or both) and a relatively small anodic current that is required to prevent repassivation and maintain locally the critical solution chemistry. This small current is produced at some distance from the depassivated region (for example by oxygen reduction or hydrogen evolution on cathodically active intermetallics, or on the auxiliary electrode during anodic polarization) and it is hereon named ‘remote’ to differentiate from the current produced by hydrogen evolution in close proximity of the corrosion front.

The source of the ‘remote’ anodic current can be either far or relatively close to the corrosion front, and its precise location is not relevant for the discussion of the model presented here. It is important, however, to point out that the model presented here is based on arguments regarding variation and distribution of currents, rather than variations of potential, which, incidentally, simplifies the mechanistic interpretation and the visualization of the corrosion process. The underlying assumptions for the discussion to be valid are that the metal supports a fast anodic kinetic (i.e. low anodic Tafel coefficient) and a comparatively slow cathodic kinetic (i.e. high cathodic Tafel coefficient); these assumptions are both verified for aluminium. The direct implications of the above assumptions are that: i) the increase in potential due to the application of an anodic current is generally small (because the anodic Tafel coefficient is small) and ii) since the increase in potential following the application of an anodic current is small, the decrease in the rate of the cathodic reaction is negligible (because of the comparatively high cathodic Tafel coefficient). Although consideration of currents simplifies substantially the mechanistic interpretation, from the physical viewpoint, all processes are driven by the locally available overpotential and limited by kinetic factors and local IR drops within the electrolyte. Thus, a variation of local current is always the consequence of a variation (whatever small) of the locally available overpotential. Such a variation of current, however, also induces a variation in the local IR drop that, in turn, induces a re-adjustment of the overpotential locally available. The overall electrode behaviour is determined by the superimposition of a large number of individual localized processes.

All the fundamental processes involved in hydrogen generation during free corrosion or polarization are schematically depicted in Fig. 1. In Fig. 1a–c, the effects associated to the availability of a ‘remote’ anodic current are graphically illustrated. In the absence of conditions that promote local depassivation (for example in the absence of chlorides), the current only induces thickening of the oxide film (Fig. 1a), as normally observed during anodizing. In the presence of chlorides, the ‘remote’ anodic current induces localized rupture of the oxide film and local formation of an aluminium chloride film. The latter is less stable compared to the aluminium oxide film and it might either be not homogeneous, such as some regions of the underlying metal are transiently exposed to the electrolyte and hydrogen evolves from the exposed metal, or be sufficiently thin for electron tunnelling, such as hydrogen can evolve from the film-solution interface (Fig. 1b). The discrimination between these two cases is not relevant for the concepts advanced here, and it is not discussed in detail. As a result of the large difference between the reversible potentials for aluminium oxidation and hydrogen evolution, at locations where depassivation has occurred, a sufficient overpotential is available and hydrogen evolution is observed (Fig. 1c). Thus, the corrosion front acts as a ‘current amplifier’, schematically depicted in Fig. 2, where a relatively small ‘remote’ anodic current is responsible for a substantial ‘local’ anodic current, associated to the formation of hydrogen streams. Overall, the total amount of oxidized metal is proportional to the sum of the ‘remote’ anodic current and the ‘local’ anodic current. The ratio between the ‘remote’ anodic current and the induced ‘local’ anodic current is unknown, and might vary significantly depending on the experimental conditions, composition and microstructure of the metal. For the

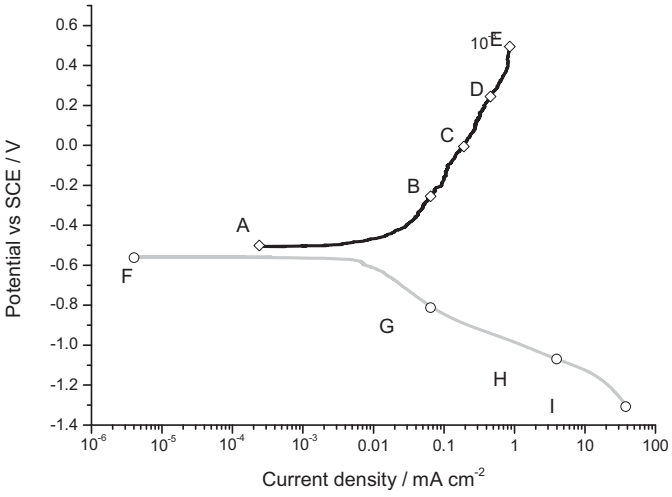

Fig. 3. Potentiodynamic polarization behaviour of aluminium in 1 M H_2SO_4.

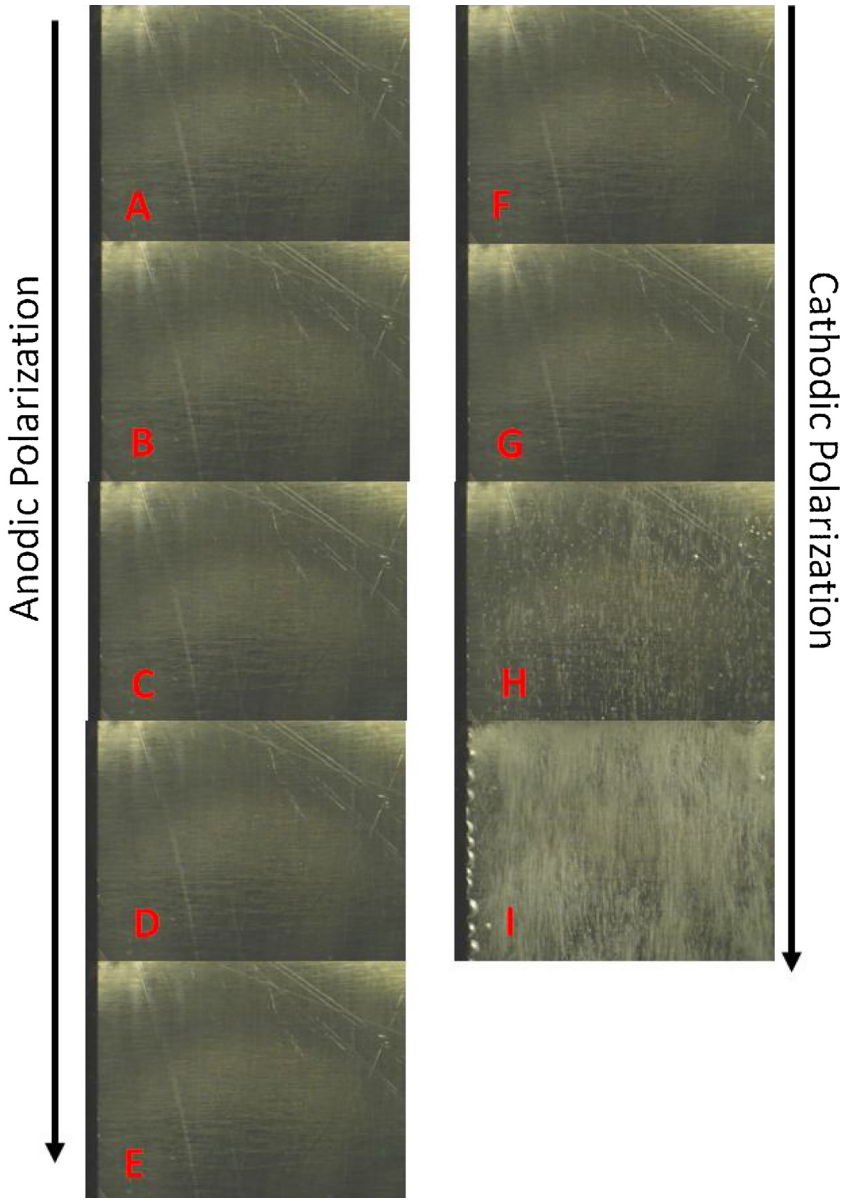

Fig. 4. Surface appearance of aluminium during polarization (anodic: A-E, cathodic: F-I) in 1 M H_2SO_4. The letters on the images correspond to the points in the polarization curve identified by the symbols in Figure 3. The sample was placed vertical in the electrochemical cell so that hydrogen streams appear as fine, discrete, vertical and lightly imaging features.

purpose of the model described here, it is not important to determine if, within the small area of the active corrosion front, there is spatial separation between the regions where oxidation of metal and hydrogen evolution occurs.

As mentioned previously, the source of the 'remote' anodic current can be either far or close to the corrosion front. In particular, it can be generated by: i) more noble intermetallic particles on the uncorroded regions (Fig. 1d), ii) pre-corroded regions (Fig. 1e), where enrichment of nobler alloying elements or increased exposure of cathodic intermetallics enhances the cathodic activity, or iii) an external circuit applying an anodic polarization (Fig. 1f), or a combination of some or all of the previous. For example, it is likely that during the early stages of corrosion the 'remote' anodic current is provided by the more noble intermetallics on the uncorroded regions and, as corrosion progresses, the contribution from the corroded that might be cathodically activated, for example due to exposure of cathodic intermetallics or enrichment of noble elements following preferential aluminium oxidation, might increase. During anodic polarization, the 'remote' anodic current is increased artificially by the external circuit, resulting in increased depassivation and consequent increased hydrogen evolution from the corrosion front. A key point of the model proposed here is that the rate of the cathodic reaction producing the 'remote' anodic current should decrease with increasing anodic polarization. On the contrary, the hydrogen evolved as a result of the increased availability of 'remote' anodic current from an external circuit, should increase with increasing anodic polarization.

Finally, the local value of the potential at the metal/electrolyte interface at the regions where the 'remote' anodic current exits deserves attention. These regions are substantially smaller compared to the regions where the 'remote' anodic current is generated. Consequently, the local current density in proximity of a small depassivated region is very high and it induces a substantial local ohmic drop. Due to this ohmic drop there is an increase in solution potential from the bulk of the electrolyte towards the sites

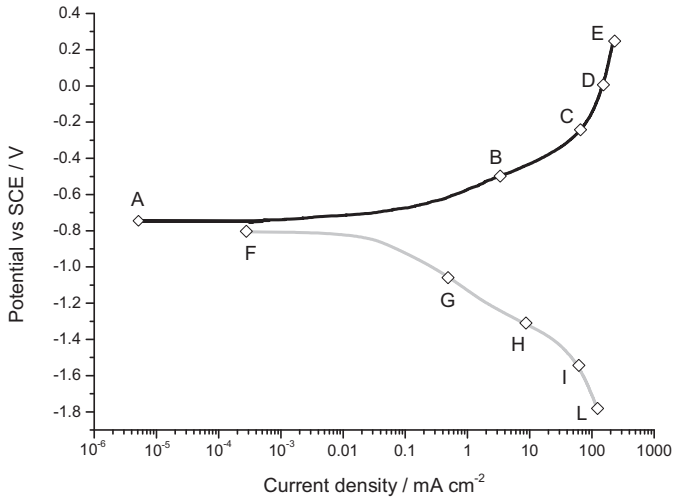

Fig. 5. Potentiodynamic polarization behaviour of aluminium in 1 M H_2SO_4 with the addition of 3.5% NaCl.

where the 'remote' anodic current exits the metal. Thus, the available potential difference at these anodic sites is such that hydrogen evolution is possible.

3. Experimental details

Aluminium electrodes were cut from large 0.9 mm thick 99.99 wt.% aluminium sheets and subsequently masked to expose a surface of 3 cm^2 ($1.5 \times 2\ cm^2$). Prior to testing, the aluminium surface was degreased by immersion in acetone for 5 min. On some of the electrodes, a self-adhesive copper tape (electrical grade copper, Agar Scientific, G253), normally used to ensure conductivity between specimens and holder during scanning electron microscopy, was applied. The electrical connection between the self-adhesive strip and the underlying aluminium was verified by measuring the resistance with a digital multimeter. Values of resistance of less than 1 ohm were considered indication of a good electrical connection between the two metals. The dimension of the exposed copper strips was $15 \times 4\ mm^2$. Potentiodynamic polarization were undertaken in 1 M H_2SO_4 with and without the addition of 3.5 wt.% NaCl, in a test solution of approximately 200 ml at room temperature by using an Iviumstat potentiostat. A typical three electrode cell configuration was used, with the aluminium specimen as working electrode, a saturated calomel electrode as reference, and a platinum mesh as the counter electrode. The images and videos were acquired by using a Maplin USB digital microscope. In order to limit the duration of the videos, a sweep rate of 5 mV s^{-1} was used. Video recording was initiated simultaneously with polarization, therefore one second in the video recording is equivalent to a potential variation of 5 mV. All the polarizations were initiated at the open circuit potential. Prior to polarization, the electrodes were immersed for approximately 3 minutes in the electrolyte. During this time, the optical system for video and image acquisition was adjusted and the surface appearance during free corrosion was recorded. For each condition a potentiodynamic anodic polarization was applied first, then the electrode was left at the corrosion potential for three minutes and, finally, a cathodic potentiodynamic polarization was recorded.

4. Results

Potentiodynamic polarizations were performed on high-purity aluminium in 1 M H_2SO_4 electrolyte, an electrolyte widely used for anodizing of aluminium [27–30]. In this electrolyte, at the open circuit potential, the aluminium oxide naturally present on the surface is partially soluble. Thus the electrolyte attacks the external regions of the oxide provoking its dissolution. However, the potential difference between the anodic reaction of aluminium oxidation and the cathodic reaction of hydrogen evolution provides the driving force for the re-growth of the oxides and, consequently the aluminium surface is always covered entirely by an oxide layer. During anodic polarization in the sulphuric acid electrolyte, the aluminium oxide film grows homogeneously on the metal surface by inward migration of oxygen anions and outward migration of aluminium cations due to the electric field generated by the applied potential across the film. Under these conditions, a porous type anodic film can form, with a barrier layer thickness that is proportional to the applied potential. The details of film growth during potentiodynamic polarization in sulphuric acid electrolyte can be found elsewhere [27].

The potentiodynamic polarization response for aluminium in the sulphuric acid electrolyte is presented in Fig. 3, where the symbols indicate the potentials associated to the images of Fig. 4. During the anodic scan, the current progressively increased to 1 mA cm^{-2} at 0.4 V SCE. Given the absence of the chloride ions, a stable oxide film over the entire metal surface was generated, no depassivation occurred, and hydrogen evolution was not observed (Fig. 4A-E, Video 1). For comparison, cathodic polarizations were also measured. It is evident from Fig. 5 H-I that, as expected for a valve metal such as aluminium, hydrogen evolution was readily revealed, with the amount of hydrogen bubbles increasing at lower electrochemical potential.

Supplementary material related to this article found, in the online version, at http://dx.doi.org/10.1016/j.electacta.2015.08.076.

Similar experiments were performed in 1 M H_2SO_4 with the addition of 3.5 % NaCl which destabilizes the film (Fig. 5, and Video 2). Due to the relatively low number of cathodic sites on the pure aluminium electrode, at the corrosion potential the 'remote' anodic current was very small, and consequently very little hydrogen evolved from the surface despite being immersed at open circuit potential for about 3 minutes. This is visible in the first photograms of Video 2 as well as in Fig. 6A. However, during anodic polarization, the value of current density was substantially higher than that measured in the absence of chlorides, indicating that the oxide film was locally ruptured (rather than homogeneously thickened). Abundant hydrogen evolution was observed during anodic polarization (Fig. 6B-E). Furthermore, during the early stages of polarization, it was possible to observe the formation of hydrogen streams (Fig. 6B and Video 2) corresponding to the active corrosion sites. Immediately after termination of the anodic polarization, the hydrogen streams disappeared (Video 2, after 3′ 20″). Similarly to the measurements in the absence of chlorides, as expected, hydrogen evolution was observed during cathodic polarization (Fig 7F-L) and the cathodic polarization branches in either environment, with or without chlorides, were comparable.

Supplementary material related to this article found, in the online version, at http://dx.doi.org/10.1016/j.electacta.2015.08.076.

A third set of experiments was performed in the chloride containing environment but on aluminium electrodes where a small strip of self-adhesive copper tape was applied (Figs. 8–9). During the initial free corrosion, hydrogen bubbles developed mainly from the copper strip indicating that a significant 'remote' anodic current was made available for depassivation (Fig. 7, Video 3). It is of interest to note that, although the abundant hydrogen evolution on copper indicated that cathodic activity of the aluminium-copper electrode was clearly higher than that on the aluminium electrode, the free corrosion potentials for the two cases were very similar and within

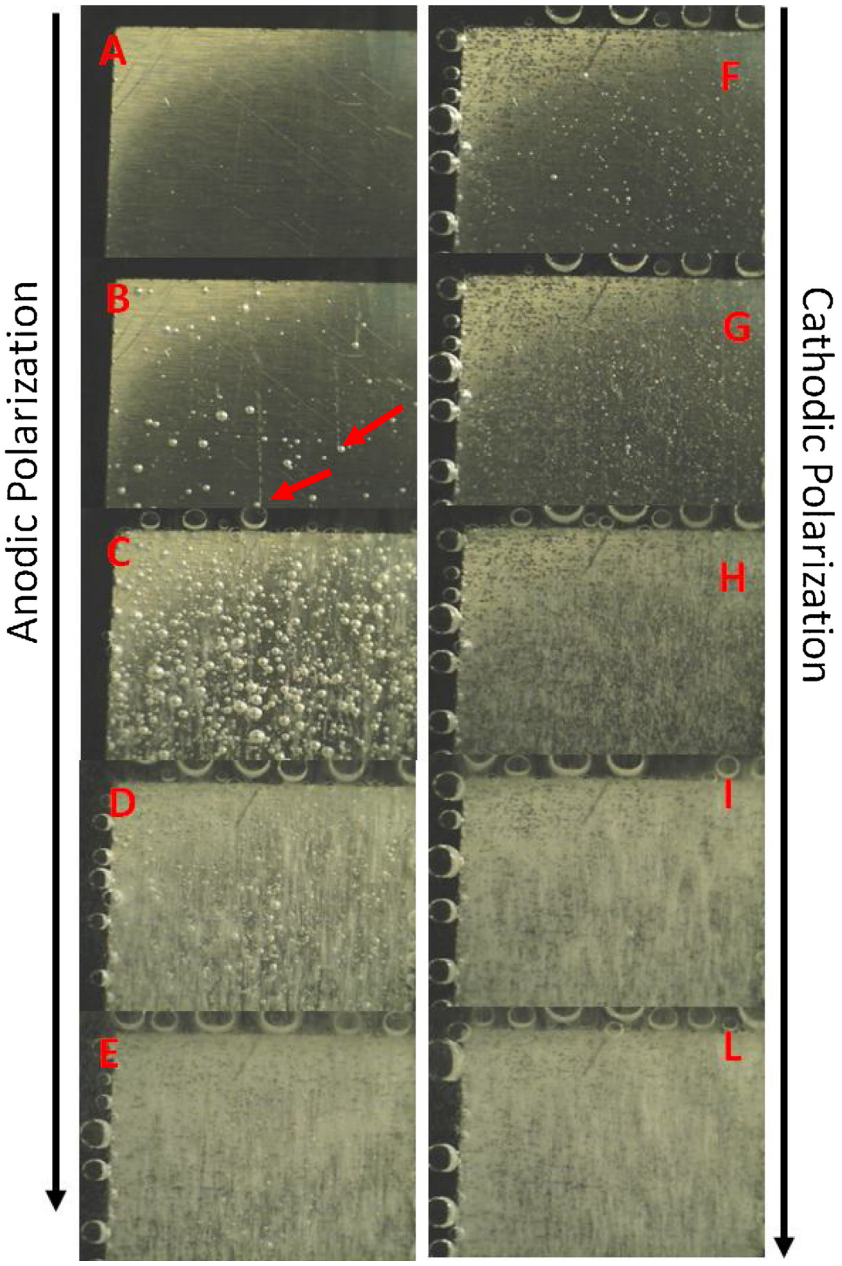

Fig. 6. Surface appearance of aluminium during polarization (anodic: A-E, cathodic: F-L) in 1 M H_2SO_4 with the addition of 3.5% NaCl. The letters on the images correspond to the points in the polarization curve identified by the symbols in Fig. 5. The red arrows indicates the locations of the first hydrogen streams. The sample was placed vertical in the electrochemical cell so that hydrogen streams appear as fine, discrete, vertical and lightly imaging features. Coarser and more stable hydrogen bubbles are also clearly visible.

the natural variations between repeated experiments. This indicates that the assumptions on the effects of current variations on the electrode potential illustrated earlier, and at the basis of the model presented here, are valid for this system. On the aluminium surface, a limited number of stable hydrogen bubbles were generated immediately after immersion, but after about 40 seconds hydrogen streams appeared (Video 3, bottom left, after 40″). When the aluminium-copper electrode was anodically polarized (Figs. 8–9, Video 4), the hydrogen evolution from the copper decreased and the large majority of the hydrogen developed from the aluminium surface. Hydrogen streams were evident over the entire surface. Immediately after interruption of the anodic polarization (Video 4, after 3′ 15″), the hydrogen restarted to evolve mainly from the copper surface. During cathodic polarization (Fig. 9F-G), the large majority of the hydrogen developed from the copper surface.

Supplementary material related to this article found, in the online version, at http://dx.doi.org/10.1016/j.electacta.2015.08.076.

5. Discussion

The solubility and the stability of aluminium oxide can easily be modified such as that the oxide is soluble but stable, i.e. as it dissolves in the outer regions it reform in the inner regions, or it is locally disrupted. In the absence of depassivating ions, when an anodic potentiodynamic polarization is applied, the oxide film thickens without hydrogen evolution since the metal is never exposed directly to the electrolyte. Conversely, under conditions

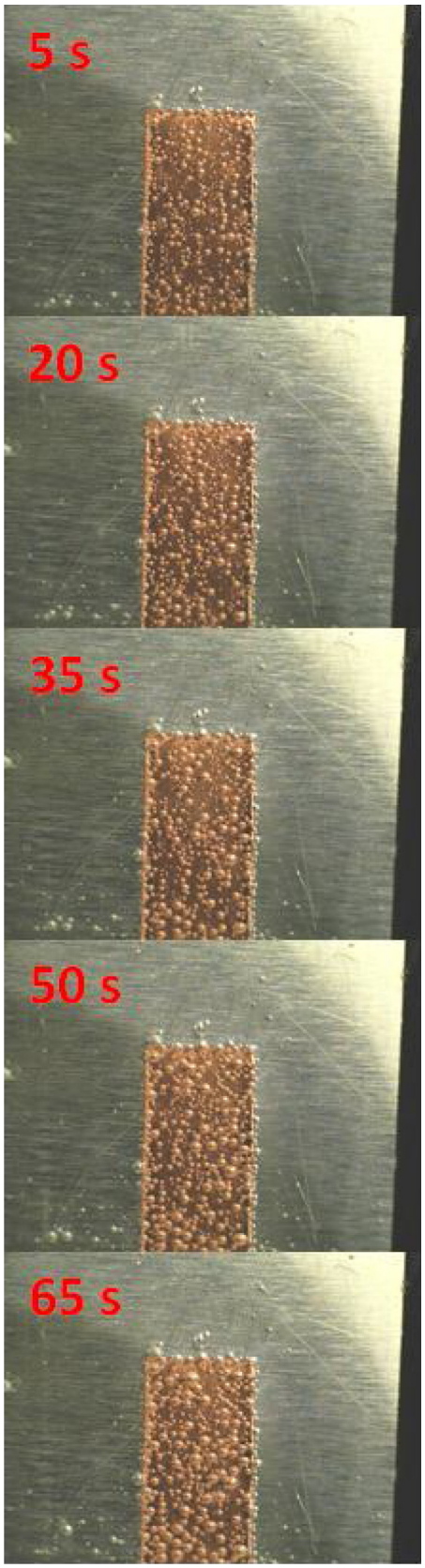

Fig. 7. Surface appearance of aluminium galvanically coupled with copper during free corrosion in 1 M H_2SO_4 with the addition of 3.5% NaCl. The immersion time is indicated on the images. The sample was placed vertical in the electrochemical cell so that hydrogen streams appear as fine, discrete, vertical and lightly imaging features.

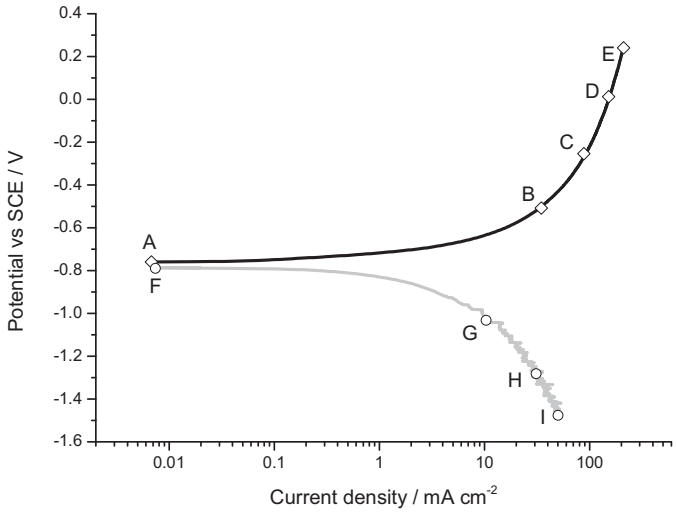

Fig. 8. Potentiodynamic polarization behaviour of aluminium galvanically coupled with copper in 1 M H_2SO_4 with the addition of 3.5% NaCl.

where local depassivation is possible, such as for example in the presence of chlorides, the current produced during free corrosion by the cathodic sites does not produce a uniform oxide film growth everywhere on the metal surface, but results mainly in local depassivation. At these active locations, where the oxide is disrupted, a relatively instable and thin aluminium chloride salt film develops and, as a result, either some locations of the metal are directly exposed to the electrolyte, or electron tunnelling is possible across the thin film. In both cases, hydrogen evolution can take place due to the large difference between the low potential present at the dissolving aluminium interface and the comparatively high reversible potential for hydrogen evolution. The hydrogen bubbles that develop from the active anodic regions are very small, since the substrate on which they form is rapidly consumed by the anodic reaction and therefore it cannot provide anchoring. Such small bubbles form the hydrogen streams observed. Given that on pure aluminium there are little cathodic sites, the 'remote' anodic current is limited and so is the hydrogen evolution observed at the corrosion potential, even in the chloride containing environment. During anodic polarization, the 'remote' anodic current is made available by the external circuit. As a result, the passivity is compromised on an increasing number of locations and an increase in hydrogen evolution is observed (negative difference effect).

The 'remote' anodic current can also be provided during free corrosion by galvanic coupling with copper, mimicking the effect of intermetallics or precorroded regions. Unlike for a practical alloy where the cathodically active particles are small, by using this macroscopic model system, it is possible to identify, both during free corrosion and during anodic polarization, the regions where the 'remote' anodic current is produced by hydrogen evolution (the copper) from the regions where the 'local' anodic current is produced by hydrogen evolution at the corrosion front (the aluminium). It is evident that, at the corrosion potential, hydrogen evolution is favoured on copper that is nobler. Importantly, the bubbles generated on copper do not form streams, but grow for a prolonged period of time before detaching from the surface. This is due to the fact that the copper surface is stable and the substrate under the growing bubble is not consumed, allowing the bubble to anchor and grow. The hydrogen evolution on copper generates sufficient 'remote' anodic current to induce depassivation at some location and initiation of corrosion on aluminium. Where this happens, hydrogen streams are generated, and a substantial 'local'

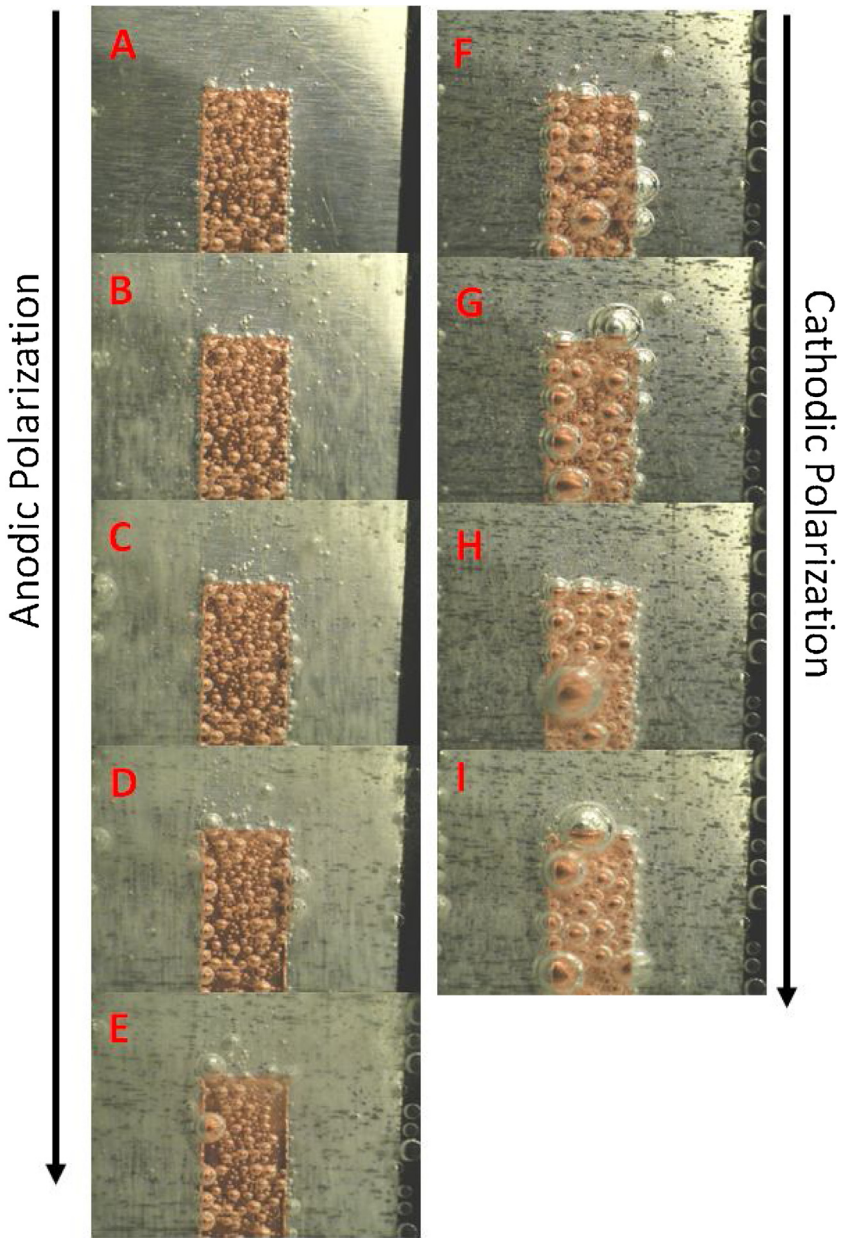

Fig. 9. Surface appearance of aluminium galvanically coupled with copper during polarization (anodic: A-E, cathodic: F-I) in 1 M H_2SO_4 with the addition of 3.5% NaCl. The letters on the images correspond to the points in the polarization curve identified by the symbols in Figure 8.

anodic current is generated at the corrosion site, due to hydrogen evolution. During anodic polarization, the hydrogen evolution from copper decreases, as expected from usual electrochemical theory, but increases on aluminium, due to the local depassivation due to increased 'remote' anodic current provided by the external circuit. When the anodic polarization is terminated, i.e. the additional 'remote' anodic current provided by the circuit is removed, copper becomes again the main source of 'remote' anodic current and hydrogen evolution on the copper surface is reinitiated immediately.

6. Summary

In this work, a model has been proposed to account for the increased hydrogen evolution during anodic polarization. The model is based on the assumption that local depassivation results in hydrogen evolution at the active anodic site due to the large potential difference between aluminium oxidation and hydrogen evolution and due to the poorly protective properties of the salt film (if any) developed at this site. The depassivation is promoted and sustained by the presence of chlorides and of a 'remote' anodic current provided by cathodically active regions, such as intermetallics or precorroded areas, or by an external circuit. Overall, the corrosion front acts as a current amplifier, where a 'remote' anodic current induces the oxidation of a comparatively large amount of metal. The experimental observations on the model system based on aluminium and aluminium galvanically coupled with copper, polarized in sulphuric acid in the presence and absence of chlorides, were in good agreement with the proposed interpretation.

Acknowledgements

EPSRC is acknowledged for provision of financial support through the LATEST2 Programme Grant (EP/H020047/1).Dr. A. Valota is acknowledged for valuable comments and proof reading.

References

[1] W. Zhang, G.S. Frankel, Transitions between pitting and intergranular corrosion in AA2024, Electrochim. Acta 48 (2003) 1193–1210.
[2] X. Zhou, C. Luo, T. Hashimoto, A.E. Hughes, G.E. Thompson, Study of localized corrosion in AA2024 aluminium alloy using electron tomography, Corros. Sci. 58 (2012) 299–306.
[3] R.G. Buchheit, R.P. Grant, P.F. Hiava, B. Mckenzie, G. Zender, Local Dissolution Phenomena Associated with S Phase (AI2CuMg) Particles in Aluminum Alloy 2024-13, J. Electrochem. Soc. 144 (1997) 2621–2628.
[4] H.W. Pickering, R.P. Frankenthal, ON THE MECHANISM OF LOCALIZED CORROSION OF IRON AND STAINLESS STEEL, J. Electrochem. Soc. 119 (1972) 1297–1310.
[5] C.B. Bargeron, R.C. Benson, Analysis of the Gases Evolved during the Pitting Corrosion of Aluminum in Various Electrolytes, J. Electrochem. Soc. 127 (1980) 2528–2530.
[6] S.B. de Wexler, J.R. Galvele, ANODIC BEHAVIOR OF ALUMINUM STRAINING AND A MECHANISM FOR PITTING, J. Electrochem. Soc. 121 (1974) 1271–1276.
[7] D.M. Dražić, J. Popić, Hydrogen evolution on aluminium in chloride solutions, J. Electroanal. Chem 357 (1993) 105–116.
[8] D.M. Dražić, J.P. Popić, Z. Rakočević, Real surface area of the aluminium electrode in sodium chloride solution, J. Serb. Chem. Soc. 64 (1999) 685–693.
[9] G.S. Frankel, The growth of 2-D pits in thin film aluminum, Corros. Sci. 30 (1990) 1203–1218.
[10] D.M. Dražić, J.P. Popić, Corrosion rates and negative difference effects for Al and some Al alloys, J. Appl. Electrochem. 29 (1999) 43–50.
[11] A.R. Despić, D.M. Dražić, M.M. Purenović, N. Ciković, Electrochemical properties of aluminium alloys containing indium, gallium and thallium, J. Appl. Electrochem 6 (1976) 527–542.
[12] I.D. Zartsyn, V.M. Samartsev, I.K. Marshakov, The kinetics of hydrogen evolution and the change of aluminium anodic potential under chloride-ion activation, Zashchita Metallov 30 (1994) 45–47.
[13] G. Song, A. Atrens, Understanding magnesium corrosion. A framework for improved alloy performance, Adv. Eng. Mater. 5 (2003) 837–858.
[14] G. Song, A. Atrens, D. St, X.W. John, J.N. u, The anodic dissolution of magnesium in chloride and sulphate solutions, Corros. Sci 39 (1997) 1981–2004.
[15] G. Song, A. Atrens, D. Stjohn, J. Nairn, Y. Li, The electrochemical corrosion of pure magnesium in 1N NaCl, Corros. Sci. 39 (1997) 855–875.
[16] G.L. Song, A. Atrens, Corrosion mechanisms of magnesium alloys, Adv. Eng. Mater. 1 (1999) 11–33.
[17] G.S. Frankel, A. Samaniego, N. Birbilis, Evolution of hydrogen at dissolving magnesium surfaces, Corros. Sci. 70 (2013) 104–111.
[18] G. Williams, N. Birbilis, H.N. McMurray, The source of hydrogen evolved from a magnesium anode, Electrochem. Commun. 36 (2013) 1–5.
[19] M. Curioni, The behaviour of magnesium during free corrosion and potentiodynamic polarization investigated by real-time hydrogen measurement and optical imaging, Electrochim. Acta 120 (2014) 284–292.
[20] M. Curioni, F. Scenini, T. Monetta, F. Bellucci, Correlation between electrochemical impedance measurements and corrosion rate of magnesium investigated by real-time hydrogen measurement and optical imaging, Electrochim. Acta 166 (2015) 372–384.
[21] M.E. Straumanis, Uncommon Valency Ions and the Difference Effect, J. Electrochem. Soc. 105 (1958) 284–286.
[22] G.A. Marsh, E. Schaschl, The Difference Effect and the Chunk Effect, J. Electrochem. Soc. 107 (1960) 960–965.
[23] M.E. Straumanis, Valency of Ions Formed during Anodic Dissolution of Metals in Acids TECHNICAL PAPERS, J. Electrochem. Soc. 108 (1961) 1087–1092.
[24] J.P. Popić, M. Avramov-Ivić, D.M. Dražić, Ring detection of hydrogen evolution on a rotating disc-ring electrode, J. Serb. Chem. Soc. 61 (1996) 1233–1240.
[25] G.S. Frankel, S. Fajardo, B.M. Lynch, Introductory lecture on corrosion chemistry: a focus on anodic hydrogen evolution on Al and Mg, Faraday Discuss 180 (2015) 11–33.
[26] M. García-Rubio, P. Ocón, M. Curioni, G.E. Thompson, P. Skeldon, A. Lavía, I. García, Degradation of the corrosion resistance of anodic oxide films through immersion in the anodising electrolyte, Corros. Sci. 52 (2010) 2219–2227.
[27] M. Curioni, P. Skeldon, G.E. Thompson, Anodizing of aluminum under nonsteady conditions, J. Electrochem. Soc. 156 (2009) C407–C413.
[28] M. Curioni, E.V. Koroleva, P. Skeldon, G.E. Thompson, Flow modulated ionic migration during porous oxide growth on aluminium, Electrochim. Acta 55 (2010) 7044–7049.
[29] Y. Ma, X. Zhou, G.E. Thompson, M. Curioni, T. Hashimoto, P. Skeldon, P. Thomson, M. Fowles, Anodic film formation on AA 2099-T8 aluminum alloy in tartaric-sulfuric acid, J. Electrochem. Soc. 158 (2011) C17–C22.
[30] Y. Ma, X. Zhou, G.E. Thompson, M. Curioni, X. Zhong, E. Koroleva, P. Skeldon, P. Thomson, M. Fowles, Discontinuities in the porous anodic film formed on AA2099-T8 aluminium alloy, Corros. Sci. 53 (2011) 4141–4151.